C. R. Physique 14 (2013) 601–606

Contents lists available at SciVerse ScienceDirect

Comptes Rendus Physique

www.sciencedirect.com

Trends and perspectives in solid-state wetting / Mouillage solide–solide : tendances et perspectives

# Interfacial reaction during dewetting of ultrathin silicon on insulator

## *Réaction interfaciale au cours du démouillage de films ultrafins de silicium sur un isolant*

Koichi Sudoh [a,*], Muneyuki Naito [b]

[a] *The Institute of Scientific and Industrial Research, Osaka University, 8-1 Mihogaoka, Ibaraki, Osaka 567-0047, Japan*
[b] *Department of Chemistry, Konan University, Okamoto, Higashinada, Kobe, Hyogo 658-8501, Japan*

A R T I C L E I N F O

*Article history:*
Available online 31 July 2013

*Keywords:*
Interfacial reaction
Dewetting
Nanocrystal
Silicon on insulator

*Mots-clés :*
Réaction interfaciale
Démouillage
Nanocristal
Silicium sur isolant

A B S T R A C T

We have studied the $Si/SiO_2$ interfacial reaction during solid-state dewetting of 7-nm-thick Si(001) ultrathin films on $SiO_2$ substrates. Immediately after formation of Si nanocrystals at the dewetting front, $Si/SiO_2$ interface depression occurs at the edge of the nanocrystal because of the interfacial reaction. By examining the $Si/SiO_2$ interface morphology for nanocrystals at different distances from the dewetting front, we found that the interface depth increases linearly with time. We also estimated that the effective activation energy for the interfacial depression is about 3.9 eV. Furthermore, we explain the effect of the interfacial reaction on the active morphological change involved in dewetting front propagation.

© 2013 Académie des sciences. Published by Elsevier Masson SAS. All rights reserved.

R É S U M É

Cet article s'intéresse à la réaction interfaciale $Si/SiO_2$ pendant le démouillage solide–solide de films ultrafins de Si(001) de 7 nm d'épaisseur sur des substrats de $SiO_2$. Immédiatement après formation de nanocristaux de silicium au front de démouillage, une dépression au niveau de l'interface $Si/SiO_2$ survient sur le bord du nanocristal à cause de la réaction interfaciale. En examinant la morphologie de l'interface $Si/SiO_2$ pour des nanocristaux situés à différentes distances du front de démouillage, nous mettons en évidence une croissance linéaire de la profondeur de l'interface avec le temps. Nous avons aussi estimé l'énergie d'activation effective de la dépression interfaciale à environ 3,9 eV. De plus, nous expliquons l'effet de la réaction interfaciale sur le changement morphologique actif impliqué dans la propagation du front de démouillage.

© 2013 Académie des sciences. Published by Elsevier Masson SAS. All rights reserved.

## 1. Introduction

Silicon on insulator (SOI) is a well-established composite material, widely used in high-performance microelectronic devices. When ultrathin SOI substrates are annealed at high temperature in oxygen-free atmospheres, solid-state dewetting of

* Corresponding author.
*E-mail address:* sudoh@sanken.osaka-u.ac.jp (K. Sudoh).

1631-0705/$ – see front matter © 2013 Académie des sciences. Published by Elsevier Masson SAS. All rights reserved.
http://dx.doi.org/10.1016/j.crhy.2013.06.008

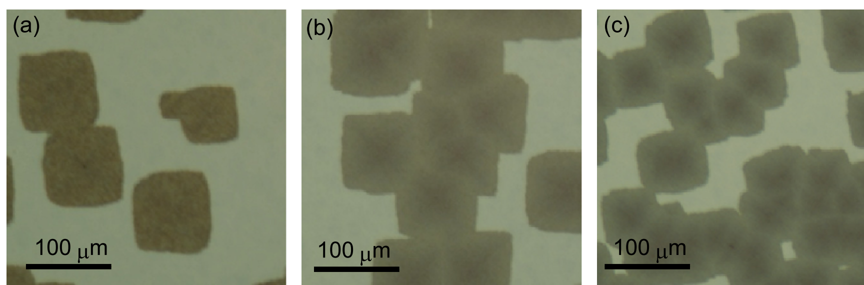


**Fig. 1.** Optical images showing dewetted regions on 7-nm-thick SOI samples. The annealing conditions are (a) 800 °C for 6 min, (b) 900 °C for 15 s, and (c) 950 °C for 5 s. Color available online.

the ultrathin Si film occurs, forming an array of Si nanocrystals [1–11]. Solid-state dewetting is understood to be a morphological change via surface diffusion, which reduces the total of the surface and interface free energy [12–14]. Recently, the dynamics of dewetting on SOI systems have been actively studied because of the potential application of self-organized Si nanocrystals in various electronic devices.

The other important phenomenon that occurs during high-temperature annealing of SOI is thermal decomposition of $SiO_2$ at the Si/$SiO_2$ interface. The Si–$SiO_2$ system is chemically unstable and the interfacial reaction $Si + SiO_2 \rightarrow 2SiO$ (g) occurs at high temperatures [15]. It is well known that thin $SiO_2$ films formed on Si substrates sublimate in the form of SiO during high-temperature annealing [16–20]. However, the role of the Si/$SiO_2$ interfacial reaction in dewetting of SOI systems has not been sufficiently understood, although several theoretical works [12,21] have discussed the effect of sublimation on dewetting.

Previously, we investigated the interfacial reaction between Si nanocrystals and $SiO_2$ during high-temperature annealing of 20-nm-thick ultrathin SOI substrates in ultrahigh vacuum [22]. We observed that Si nanocrystal/$SiO_2$ interfaces are much more reactive than interfaces of wetting Si films. During the reaction at the Si nanocrystal/$SiO_2$ interface, removal of O atoms from the $SiO_2$ side of the interface occurs with the remaining Si atoms incorporated into the Si nanocrystal, resulting in a depression of the interface. From the observations, we proposed that the interfacial reaction advances via O out-diffusion from $SiO_2$ into the Si island, O lateral diffusion along the interface, SiO formation at the edge of the Si island, and SiO desorption from the surface. In our previous work, we only investigated the interfacial reaction at a fairly high temperature of 1050 °C, where the reaction is rather active and a significant amount of Si atoms are evaporated as SiO during dewetting.

The present work focuses on the interfacial reaction at a lower temperature range between 750 and 900 °C, where we usually perform the self-organized formation of Si nanocrystals. We observe the Si/$SiO_2$ interface morphology in dewetted regions formed on 7-nm-thick SOI, using atomic force microscopy (AFM) and transmission electron microscopy (TEM). By analyzing the dependence of the Si/$SiO_2$ interface morphology of the Si nanocrystals on their location in the dewetted region, we reveal the time evolution of the interface morphology arising from the interfacial reaction and measure its effective activation energy. We also show the effect of interfacial reaction on the fast morphological change of the Si film involved in the propagation of the dewetting front.

## 2. Experimental

We used commercially available (001) oriented bonded SOI substrates. The thicknesses of the top Si and the buried oxide layers are 340 nm and 100 nm, respectively. The top Si layer was thinned down to approximately 7 nm by repeated cycles of thermal oxidation and chemical etching of the oxide with a dilute HF solution. The SOI samples were annealed in an ultrahigh vacuum (UHV) chamber with a base pressure of $\sim 10^{-8}$ Pa at temperatures in the 700–900 °C range. Sample heating was achieved resistively via a DC current through the sample. During annealing, the ambient pressure was usually kept below $5.0 \times 10^{-7}$ Pa. It has been shown that the dewetting behavior is dependent on the surface status of the Si film [9]. In our experiment, SOI substrates covered by native oxide were annealed in UHV to induce dewetting. The surface and Si/$SiO_2$ interface morphologies were observed by AFM and TEM. To directly observe the morphology of Si/$SiO_2$ interfaces by AFM, we used selective wet chemical etching of Si with KOH solution. The selective etching was performed at room temperature with a 7 wt.% aqueous KOH solution. According to the literature [23], in our etching conditions, the selectivity ratio between Si and $SiO_2$ is larger than ∼1000.

## 3. Results and discussion

Fig. 1 shows optical images of the 7-nm-thick SOI samples annealed at different temperatures. The samples shown in Figs. 1(a)–1(c) were annealed at 800 °C for 360 s, at 900 °C for 15 s, and at 950 °C for 5 s, respectively. Independently of the temperature, approximately square-shaped dewetted regions are formed in the SOI films. While the appearance of the dewetted region of the 800 °C-annealed sample is fairly uniform, we find a spatial gradient in contrast in the dewetted regions for annealing at 900 and 950 °C. Previously, we have reported that the interfacial reaction is more advanced from

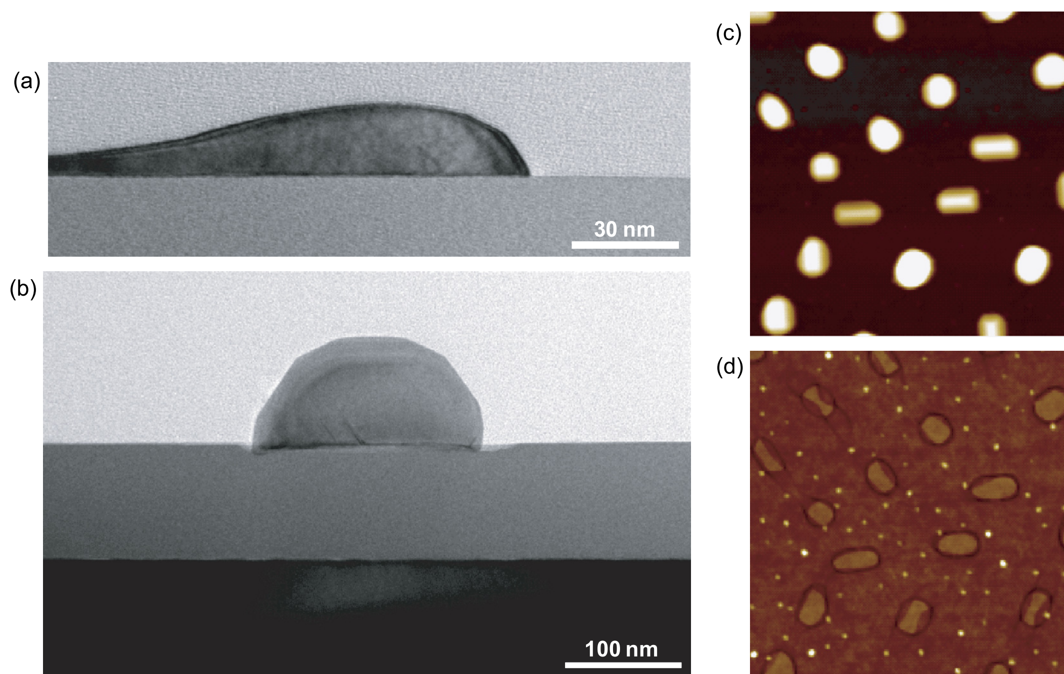


**Fig. 2.** Morphology of a 7-nm-thick SOI after annealing at 800 °C. (a, b) Cross-sectional TEM images showing the structure of (a) the thickened edge of the Si film and (b) a Si nanocrystal in a dewetted region. (c) AFM image of a dewetted region. (d) AFM image of the same region as (c) after selective wet etching of Si. The observed area is 1.5 µm × 1.5 µm. Color available online.

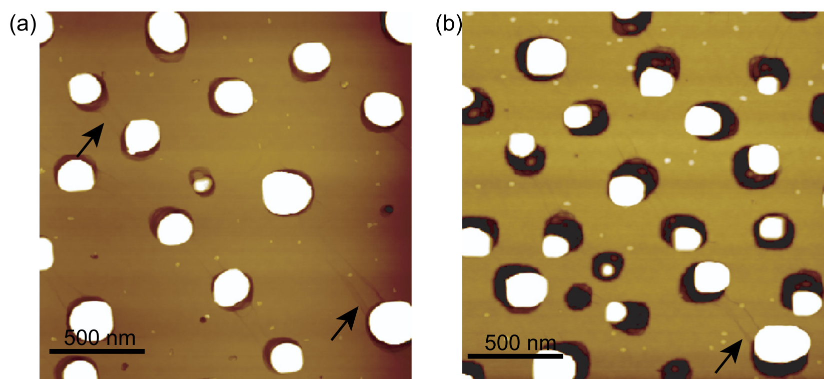


**Fig. 3.** AFM images of Si nanocrystals formed by annealing (a) at 750 °C for 120 min and (b) at 800 °C for 60 min. Color available online.

the edge towards the center of the dewetted region because the interfacial reaction is initiated at the edges of the Si nanocrystals when they are formed at the dewetting front [22]. The gradation in the optical images is because the size of the nanocrystals gradually decreases from the border toward the center of the dewetted region due to the interfacial reaction. The gradation increases with increasing temperature, showing that the influence of the interfacial reaction during dewetting becomes larger with increasing temperature.

The interfacial reaction affects the morphology during dewetting, even at lower temperatures below 800 °C. Fig. 2 shows the morphology of the dewetted region for samples annealed at 800 °C. The cross-sectional TEM images show the structures of the thickened edge of the Si film and a Si nanocrystal in the dewetted region formed by annealing at 800 °C for 5 min. We find that the bottom of the nanocrystal is slightly depressed into the underlying $SiO_2$ layer, which is the signature of the interfacial reaction [22]. Fig. 2(c) shows an AFM image of the Si nanocrystals in a dewetted region formed by annealing at 800 °C for 6 min. An AFM image of the same surface region after removing Si by selective wet etching is displayed in Fig. 2(d), where we can directly observe the Si nanocrystal/$SiO_2$ interface morphologies. We observe ringed trenches on the exposed $SiO_2$ surface. This indicates that the overall interface underneath the Si nanocrystals is not depressed, but the interface depression occurs at a localized area near the edge of the Si nanocrystal. This demonstrates that the critical process for interface depression occurs at the edge of the Si nanocrystal. Fig. 3 shows the Si nanocrystals in the dewetted regions at later stages of the interfacial reaction. Figs. 3(a) and 3(b) show the morphologies for a sample annealed at 750 °C

**Fig. 4.** The morphology of a dewetted region formed on a SOI substrate by annealing at 900 °C for 10 s. (a) 40 μm × 40 μm AFM image showing the overall dewetted region. (b–d) Magnified AFM images (2.4 μm × 2.4 μm) showing the morphology of the areas A, B, and C indicated in (a), respectively. The upper and lower panels are AFM images of the same region obtained before and after wet etching of Si, respectively. (e–g) Profiles of the ringed trenches along the lines shown in (b)–(d), respectively. Color available online.

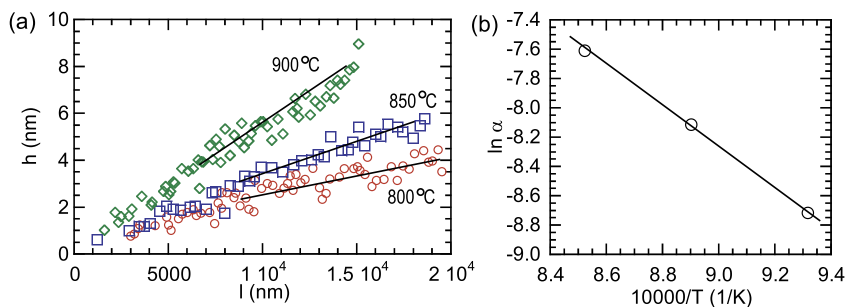


**Fig. 5.** (a) Depth $h$ of the ringed trenches observed in dewetted regions after wet chemical etching plotted as a function of the distance $l$ from the dewetting front. (b) Temperature dependence of the slope $\alpha$ measured from the $h$–$l$ plots in (a).

for 120 min and at 800 °C for 60 min, respectively. We find that the Si nanocrystals are within the pits formed by the interfacial reaction. The above-mentioned results on dewetting at the lower temperatures below 800 °C are qualitatively identical to our previous observations for dewetting at 1050 °C [22]. In Fig. 3 we also notice that there are linear grooves on the exposed $SiO_2$ surfaces as indicated by arrows. These are trails formed by the interfacial reaction in association with the nanocrystal formation in the dewetting front. The detailed process will be explained later.

To investigate the kinetics of the interface depression at the edge of Si nanocrystals, we analyzed the variation of the interface morphology of the Si nanocrystals from the dewetting front towards the center of the dewetted region. Fig. 4 shows the morphology of a dewetted region of 35 μm × 35 μm on a sample annealed at 900 °C for 10 s. Magnified AFM images of areas A, B, and C indicated in Fig. 4(a) are shown in Figs. 4(b), 4(c), and 4(d), respectively. The upper and the lower AFM images were obtained at the same region before and after selective wet etching to remove Si, respectively. In Figs. 4(e)–4(g), the profiles of the ringed grooves along the lines indicated in Figs. 4(b), 4(c), and 4(d) are shown, respectively. We find that

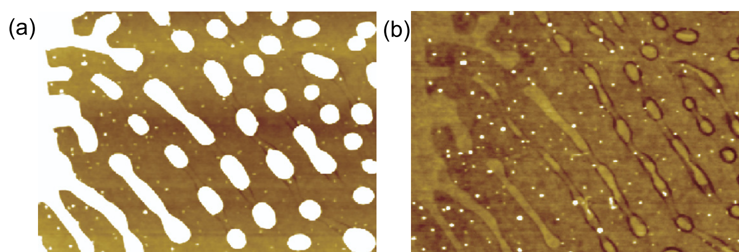


**Fig. 6.** Magnified AFM images showing the morphology of a dewetting front. AFM images (a) and (b) show morphologies before and after selective etching of Si, respectively. Color available online.

the depth of the ringed trench increases with increasing the distance from the border towards the center of the dewetted region. In Fig. 5(a), the measured trench depth $h$ is plotted as a function of the distance $l$ from the edge of the dewetted region. In Fig. 5(a), we also show the results for annealing at 800 °C for 360 s and annealing at 850 °C for 60 s. We find that $h$ is approximately proportional to $l$. The interfacial reaction begins as the Si nanocrystal is formed at the dewetting front. As the dewetting front propagates at a constant velocity $v_{\mathrm{edge}}$, the duration $\tau$ after the formation of the Si nanocrystal linearly increases with the distance $l$, as $\tau = l/v_{\mathrm{edge}}$. Thus we conclude that the Si/$SiO_2$ interface of the nanocrystal edge is depressed at a constant rate.

We find that the slope $\alpha = \mathrm{d}h/\mathrm{d}l$ for the $h$–$l$ plots in Fig. 5(a) decreases as the temperature does. The rate of the interface depression is written as $r = \mathrm{d}h/\mathrm{d}\tau = \alpha v_{\mathrm{edge}}$. Here we assume Arrhenius-type temperature dependences for $r$ and $v_{\mathrm{edge}}$: $r = r_0 \exp(-E_{\mathrm{r}}/kT)$ and $v_{\mathrm{edge}} = v_0 \exp(-E_{\mathrm{d}}/kT)$, where $E_{\mathrm{r}}$ and $E_{\mathrm{d}}$ are the effective activation energies for the interface depression and the dewetting front propagation, respectively. Then we can write the temperature dependence of $\alpha$ as $\alpha = \alpha_0 \exp(-\Delta E/kT)$, where $\Delta E = E_{\mathrm{r}} - E_{\mathrm{d}}$ and $\alpha_0 = r_0/v_0$. In Fig. 5(b), $\ln \alpha$ is plotted as a function of $1/T$. From the slope, the difference in the effective activation energy is evaluated as $\Delta E = 1.2$ eV. Previously, the effective activation energy of the dewetting front's propagation was measured to be $E_{\mathrm{d}} \sim 2.7$ eV for SOI with a thickness of $6 \pm 2$ nm [9]. Thus we estimate the effective activation energy for the interfacial reaction to be $E_{\mathrm{r}} \sim 3.9$ eV. This activation energy is comparable to that for void growth in oxide thin films on Si [20]. The reaction-induced interface depression involves oxygen diffusion in the Si nanocrystal along the interface. The activation energy for oxygen diffusion in Si is known to be 2.53 eV [24,25], which is obviously smaller than the value of $E_{\mathrm{r}}$ that we measured. For the annealing conditions, the widths of the region where the interface depression occurs are ∼50 nm. Using the reported value of oxygen diffusivity in Si [24,25], we find that the diffusion times required for a diffusion length of 50 nm are 130 s, 39 s, and 13 s at 800, 850, and 900 °C, respectively. These diffusion times are smaller than or comparable to the annealing times in the experiment. Thus we consider that the rate-limiting process for the Si/$SiO_2$ interface depression is not oxygen diffusion, but the chemical process at the edge of the nanocrystal.

In addition to the interface depression that occurs at the rather stable edges of Si nanocrystals, the interface reaction affects the morphological evolution through the active morphological change of the Si film, in association with the propagation of the dewetting front. Fig. 6 shows the magnified AFM images of a dewetting front before and after wet etching to remove Si. We find that the interface depression also occurs at the side edges of the elongated Si fingers in the dewetting front. This forms characteristic linear trails between the Si nanocrystals on the exposed $SiO_2$. Once pinch off of the Si finger occurs, fast morphological relaxation of the disconnected Si finger into a nanocrystal with a more energetically preferable shape occurs without causing significant interface depression at the Si edge. Thus the characteristic trails remain on the exposed $SiO_2$ surface.

In Fig. 6(b), we can clearly distinguish the border of the dewetted region on the samples after selective etching. The height of the $SiO_2$ surface exposed by dewetting is 0.5–0.7 nm lower than that of the outside of the dewetted region. This implies that slight etching of the $SiO_2$ layer occurs even when the $SiO_2$ surface is exposed through the fast receding of the Si film, as occurs during the propagation of the dewetting front.

## 4. Conclusion

We investigated the interfacial reaction involved in the dewetting of 7-nm-thick ultrathin SOI films. The Si/$SiO_2$ interface depression occurs in the vicinity of the edge of the Si nanocrystals and the interface depth increases linearly with time. We estimated the effective activation energy for the interface depression of Si nanocrystals to be about 3.9 eV. This result suggests that the rate-limiting process for the interface depression in the 800–900 °C temperature range is not oxygen diffusion in Si, but the reaction at the edge of the Si nanocrystal. We also showed that the interfacial reaction affects the morphological evolution in association with the active motion of Si film edges in the dewetting front.

**Acknowledgement**

The authors thank M. Nakao for the fruitful discussions they have had with him and for providing us with SOI samples.

## References

[1] Y. Ono, M. Nagase, M. Tabe, Y. Takahashi, Jpn. J. Appl. Phys. 34 (1995) 1728–1735.
[2] R. Nuryadi, Y. Ishikawa, M. Tabe, Appl. Surf. Sci. 159–160 (2000) 121.
[3] B. Legrand, V. Agache, J.P. Nys, V. Senez, D. Stievenard, Appl. Phys. Lett. 76 (2000) 3271.
[4] R. Nuryadi, Y. Ishikawa, Y. Ono, M. Tabe, J. Vac. Sci. Technol. B 20 (2002) 167–172.
[5] B. Legrand, V. Agache, T. Mélin, J.P. Nys, V. Senez, D. Stiévenard, J. Appl. Phys. 91 (2002) 106–111.
[6] B. Yang, P. Zhang, D.E. Savage, M.G. Lagally, G. Lu, M. Huang, F. Liu, Phys. Rev. B 72 (2005) 235413.
[7] D.T. Danielson, D.K. Sparacin, J. Michel, L.C. Kimerling, J. Appl. Phys. 100 (2006) 083507.
[8] P. Sutter, W. Ernst, Y.S. Choi, E. Sutter, Appl. Phys. Lett. 88 (2006) 141924.
[9] F. Cheynis, E. Bussmann, F. Leroy, T. Passanate, P. Müller, Phys. Rev. B 84 (2011) 245439.
[10] E. Bussmann, F. Cheynis, F. Leroy, P. Müller, O. Pierre-Louis, New J. Phys. 13 (2011) 043017.
[11] M. Aouassa, L. Favre, A. Ronda, H. Maaref, I. Berbezier, New J. Phys. 14 (2012) 063038.
[12] D. Srolovitz, S. Safran, J. Appl. Phys. 60 (1986) 2555.
[13] E. Dornel, J.-C. Barbé, F. de Crécy, G. Lacolle, J. Eymery, Phys. Rev. B 73 (2006) 115427.
[14] O. Pierre-Louis, A. Chame, Y. Saito, Phys. Rev. Lett. 103 (2009) 195501.
[15] J.J. Lander, J. Morrison, J. Appl. Phys. 33 (1962) 2089.
[16] R. Tromp, G.W. Rubloff, P. Balk, F.K. LeGoues, E.J. van Loenen, Phys. Rev. Lett. 55 (1985) 2332.
[17] M. Liehr, J.E. Lewis, G.W. Rubloff, J. Vac. Sci. Technol. A 5 (1987) 1559.
[18] K.E. Johnson, T. Engel, Phys. Rev. Lett. 69 (1992) 339.
[19] N. Miyata, H. Watanabe, M. Ichikawa, Phys. Rev. Lett. 84 (2000) 1043.
[20] H. Hibino, M. Uematsu, Y. Watanabe, J. Appl. Phys. 100 (2006) 113519.
[21] A. Chame, O. Pierre-Louis, Phys. Rev. E 85 (2012) 011602.
[22] K. Sudoh, M. Naito, J. Appl. Phys. 108 (2010) 083520.
[23] H. Seidel, L. Csepregi, A. Heuberger, H. Baumgärtel, J. Electrochem. Soc. 137 (1990) 3612–3626.
[24] S. Lee, D. Nichols, Appl. Phys. Lett. 47 (1985) 1001–1003.
[25] R.C. Newman, J. Phys. Condens. Matter 12 (2000) R335–R365.